Observation of spectral structures in the flux of cosmic ray protons with CALET on the International Space Station

Kazuyoshi Kobayashi[a,b,]* **and Pier Simone Marrocchesi**[c,d] **for the CALET Collaboration**

(a complete list of authors can be found at the end of the proceedings)

a InstitutionWaseda Research Institute of Science and Enginnearing, Waseda University, 17 Kikuicho, Shinjuku, Tokyo162-0044, Japan
Street number, City, Country

b JEM Utilization Center, Human Spaceflight Technology Directorate, Japan Aerospace Exploration Agency, 2-1-1 Sengen, Tsukuba, Ibaraki 305-8505, Japan

c Dept. Of Physical Sciences, Earth and Environment, Univ. Of Siena, 53100 Siena, Italy

d INFN Sezione di Pisa, Polo Fibonacci, Largo B. Pontecorvo, 3-56127 Pisa, Italy

E-mail: kenkou@aoni.waseda.jp, marrocchesi@pi.infn.it

A precise measurement of the cosmic-ray proton spectrum is carried out with the Calorimetric Electron Telescope (CALET) and a sharp softening of the energy spectrum above 10 TeV is observed. CALET, located on the International Space Station, has started data taking in October 2015 and has accumulated data for more than seven years without any serious troubles. CALET is pursuing the direct measurement of the main components of high energy cosmic rays up to ~1 PeV in order to understand the cosmic ray acceleration and propagation. Thanks to the thick calorimeter that corresponds to 30 radiation lengths and to ~1.3 proton interaction lengths, the proton analysis presented in this paper spans a broad energy range from 50 GeV to 60 TeV. Proton energy resolution is 30-40%, and the residual background is less than 10% in the E < 10 TeV region. In the multi-TeV region, we observed a spectral softening with a spectral index change from -2.6 to -2.9 in addition to the spectral hardening we had previously confirmed with a high significance above a few hundred GeV. The transition to the softer regime is much sharper than the smooth onset of hardening observed at lower energy.

ICRC2023
38th International Cosmic Ray Conference
The Astroparticle Physics Conference

---

*Speaker

1.   Introduction

Several direct measurements of cosmic-ray nuclei up to the PeV energy scale have provided insight into the general phenomenology of cosmic-ray acceleration and propagation in the Galaxy. A possible charge-dependent cutoff in the spectra is hypothesized to explain the all-nuclei spectrum. A spectral hardening has been observed for several nuclei around a few hundreds GeV per nucleon. In the case of proton, we reported the observation of a spectral hardening with much higher statistics [1] than previous experiments [2][3]. Many theoretical models have been proposed to account for the spectral hardening including the presence of different cosmic ray sources, acceleration mechanisms, effect of diffusion process in the Galaxy, and their superposition. We recently reported the observation of a proton spectral softening in the energy region around 10 TeV [4] which is consistent within errors with DAMPE [5]. It is crucial to observe accurately both the spectral hardening and the softening in order to understand the detailed mechanisms of cosmic-ray acceleration and propagation in the Galaxy. In this paper, we present our improved observation of a softening of the proton spectrum above 10 TeV which can be fitted simultaneously with the hardening of the spectrum around 500 GeV by the proton analysis using CALET data with increased statistics by 21% with respect to [4].

2.   CALET detector

The CALorimetric Electron Telescope (CALET) [6], a space-based instrument optimized for the measurement of the all-electron spectrum [7][8] and equipped with a fully active calorimeter, can also measure cosmic-ray nuclei including proton in the energy range up to 1 PeV. The thickness of the calorimeter corresponds to 30 radiation lengths and to 1.3 proton interaction lengths. The CALET detector consists of a charge detector (CHD), a 3 radiation-length thick imaging calorimeter (IMC) and a 27 radiation-length thick total absorption calorimeter (TASC), with a field of view of 45° from zenith. The CHD, which identifies the charge of the incident particle, is comprised of a pair of plastic scintillator hodoscopes arranged in two orthogonal layers. The IMC is a sampling calorimeter alternating thin layers of Tungsten absorber with layers of scintillating fibers readout individually, also providing an independent charge measurement via multiple dE/dx samples. The TASC is a tightly packed lead-tungstate ($PbWO_4$) hodoscope, measuring the energy of showering particles in the detector. More than 6 orders of magnitude in the energy region are covered by the readout using four different gain ranges. Due to the wide dynamic energy range of CALET as a single instrument, we can study the detailed shape of the spectrum without the large systematic uncertainties that can be present when operating with different detectors. Detailed description of the apparatus is given in the Supplemental Material of Ref. [7].

The instrument was launched on August 19, 2015 and emplaced on the Japanese Experiment Module-Exposed Facility (JEM-EF) on the International Space Station (ISS) with an expected mission duration of more than seven years. The mission has been extended and the expected duration is nine years (or more) in total. Figure 1 shows the ISS and a schematic view of the CALET detector. Scientific observations started on October 13, 2015 and the detector operation continues without any serious impediment so far.
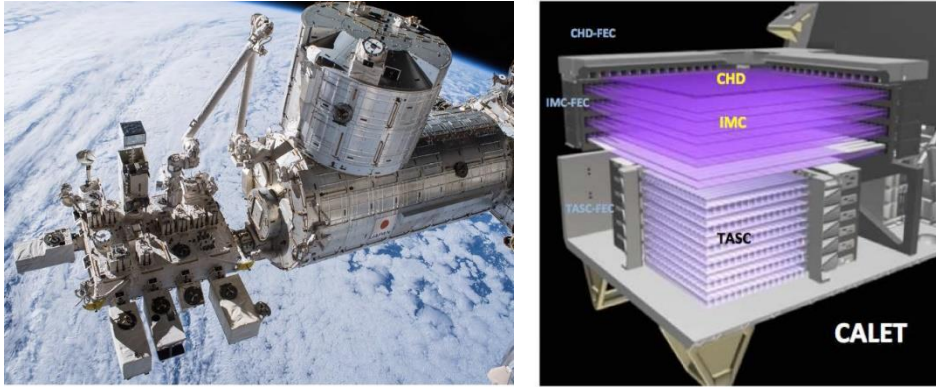
Figure 1: The ISS and CALET detector. The left figure shows the ISS. The CALET detector is located at the JEM-EF which is at the top left corner of the picture. The right figure shows a schematic view of the CALET detector.

3. Data analysis

We have analyzed the flight data collected from October 13, 2015 to April 30, 2023. The total observation live time for the HE shower trigger [6] is 1925 days and the live time fraction to total time is 84%. In addition, the low-energy (LE) shower trigger operating at a high geomagnetic latitude [6] is used to extend the energy coverage toward the lower energy region. A fiducial geometrical factor of approximately 510 cm² sr for particles penetrating CHD top to TASC bottom, with 2 cm margins at the first and the last TASC layers (acceptance A), corresponds to about 40% of the total acceptance [8]. Monte Carlo (MC) simulations reproducing the detailed detector configuration, physics processes, and detector signals, are based on the EPICS simulation package [9].

3.1 Event selection and background

In order to obtain the proton event sample, we apply the following selection criteria. We require that: (1) in the energy range, $E > 300$ GeV, the HE trigger should be asserted and the energy deposit sum of IMC 7th and 8th layers should be more than 50 minimum ionizing particles (MIPs) in both X and Y view. Also the energy deposit of TASC 1st layer should be more than 100 MIPs. In the energy range $E < 300$ GeV, the LE trigger should be asserted and the energy deposit sum of IMC 7th and 8th layers should be more than 5 MIPs in both X and Y view. Also the energy deposit of TASC 1st layer should be more than 10 MIPs. (2) Acceptance A is required as geometrical condition. (3) Kalman filter (KF) tracking in IMC should be adequate both in the X and Y view. (4) Energy deposit inside one Moliere radius along the KF track in IMC should be less than 70% of total energy deposit. (5) Off-acceptance events are removed by the following two methods. One is that the maximum fractional energy deposit in a single TASC layer should be less than 0.4. The other is that the maximum energy deposit ratio of the edge channels to the maximum channel in each TASC layer should be less than 0.4. (6) Center of gravity of TASC energy deposit in X1 and Y1 layers should be consistent with the IMC track impact point. (7)

Shower starting in IMC is required. (8) Charge is identified as proton using both CHD and IMC energy deposits. The Charge (Z) is corrected for non-linear effects as $Z = a(E)N_{\mathrm{mip}}^{b(E)/2}$, where N_{mip} is the energy deposit in MIP units and $a(E)$ and $b(E)$ are energy dependent parameters determined using the MC simulations so that the average Z is 1 for proton and 2 for helium. The selection criteria are determined to keep the efficiency at the 95% level for the lower Z side and 98% for the higher Z side. Figure 2 shows examples of the charge distribution using IMC. Criterion (4) is required to remove electron background. Criterion (5) removes particles entering from the side of the detector. Criterion (6) remove mis-reconstructed events. Details can be found in Ref. [1][4].

Background is estimated with MC simulations of cosmic ray protons, helium and electrons. After applying all the event selections, the dominant background comes from the off-acceptance protons below ~5 TeV (TASC energy deposit sum (E_{TASC})). The contamination is estimated to be less than a few percent. Above, helium is the main background source. The contamination gradually increases as the energy becomes higher and is estimated to be 20% at maximum.
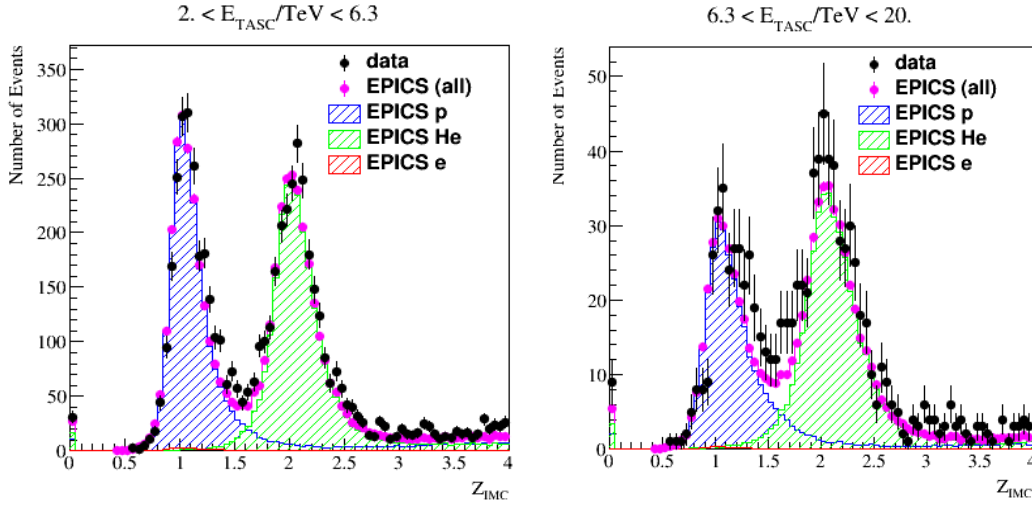

Figure 2: Charge distributions with the IMC. The left and right figures show the IMC charge for events with $2 < E_{TASC} < 6.3$ TeV and $6.3 < E_{TASC} < 20$ TeV, respectively. Data (black filled circles) is compared with MC simulations (histogram).

3.2 Energy unfolding

Figure 3 shows a proton candidate with an energy deposit of 2.9 TeV in the detector. The event example demonstrates our capability to reconstruct and identify high energy protons. Because most of protons go through the detector and the energy resolution is limited (30-40%), energy unfolding is required to estimate the primary energy distribution. It is important, therefore, to infer the detector response at the highest energies covered by the analysis. First, we build a response matrix connecting true and observed energy spectra using MC simulation. Then, we apply an iterative unfolding procedure based on Bayes theorem taking into account helium and electron background.
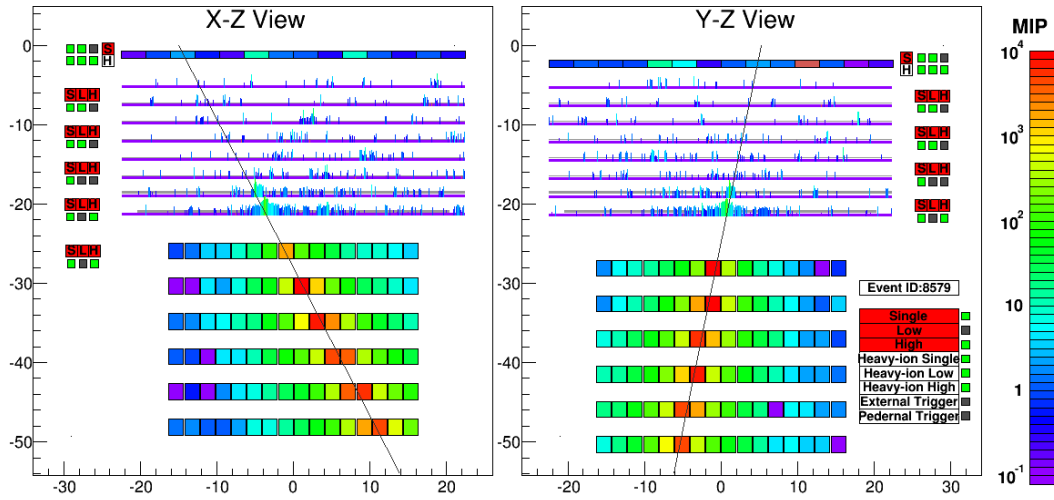
Figure 3: Proton event display with 2.9TeV energy deposit in TASC.

3.3 Systematic uncertainty

Two components are taken into account as systematic uncertainties. One is the energy independent component, 4.1% in total. It contains the uncertainties on live time (3.4%), radiation environment (1.8%), and long-term stability (1.4%). The other one is the energy dependent component, which is estimated to be less than 10% for $E < 10$ TeV. We take into account the uncertainties of MC model dependence, IMC track consistency with TASC energy deposits, shower start in IMC, charge identification, energy unfolding, and beam test configuration. For $E > 10$ TeV, the uncertainties of MC model dependence and charge identification become dominant. In the interval $10 < E < 40$ TeV the uncertainty is 20% at maximum.

3.4 Proton spectrum

Figure 4 shows the proton spectrum in the energy region from 50 GeV to 60 TeV, compared with AMS-02, CREAM-III, and DAMPE. In the low energy region with $E < 200$ GeV, the result is fully consistent. In the higher energy region, a systematic difference is observed, but the difference is within the errors. We confirmed the presence of a spectral hardening around 500 GeV with a high significance (more than 20 sigma). We also observe a spectral softening around 10 TeV. We have tested two independent analyses with different efficiencies and the two results are consistent. In order to calculate the behavior of the spectral hardening and softening quantitatively, we apply spectral fitting to the proton spectrum using a double broken power law function defined as follows:

$$\Phi' = E^{2.7} \times C \times \left(\frac{E}{1}\right)^{\gamma} \times \left(1 + \left(\frac{E}{E_0}\right)^{s}\right)^{\frac{\Delta\gamma}{s}} \times \left(1 + \left(\frac{E}{E_1}\right)^{s_1}\right)^{\frac{\Delta\gamma_1}{s_1}},$$

where Φ' is the proton flux$\times E^{2.7}$, C is the normalization factor, γ is the spectral index, $\Delta\gamma$ is the spectral variation, s is the smoothness parameter at hardening, E_0 is the hardening break energy, $\Delta\gamma_1$ is the spectral index variation due to softening, s_1 is the smoothness parameter at softening, and E_1 is the softening break energy. In figure 5, the black filled circles show the data with statistical errors and the red line shows the best fitted function. The χ^2 is 6.0 with 20 degrees of
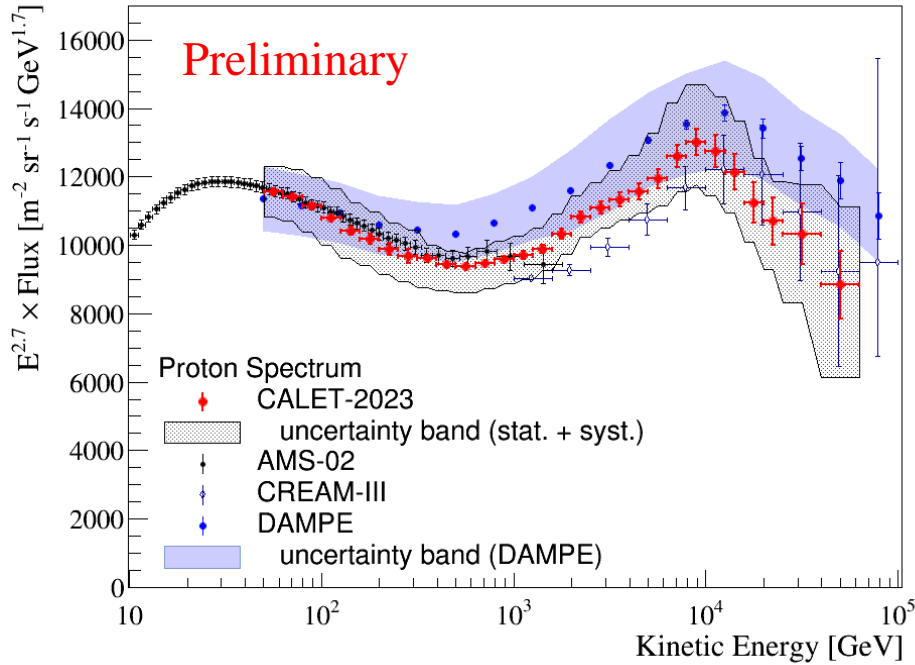

Figure 4: Proton spectrum measured by CALET (red) compared with other experiments (AMS02 [2], CREAM-III [3], and DAMPE [5]). The hatched band shows the total uncertainty for CALET. The dark blue colored band shows the total uncertainty for DAMPE.
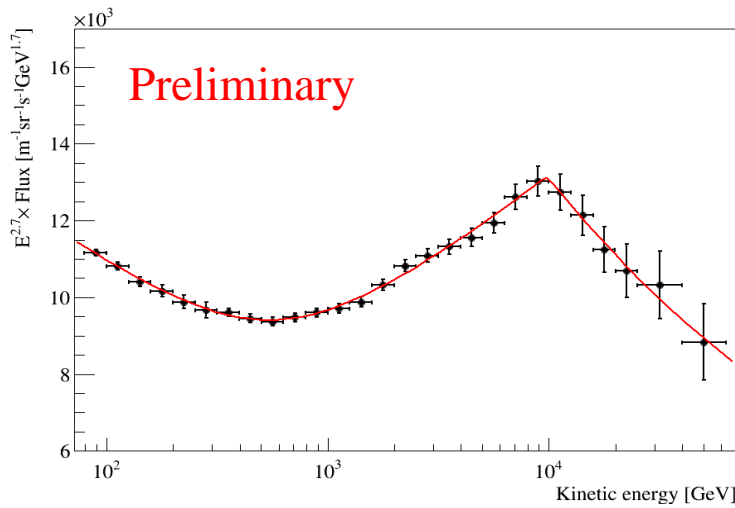

Figure 5: CALET proton spectrum fitted by a double broken power law (red solid line). The horizontal error bars are representative of the bin width.

6

freedom. The best fitted parameters are:, γ = -2.843 $\pm$ 0.005, s = 2.1$\pm$0.4, $\Delta\gamma$ = (2.9$\pm$0.1)$\times 10^{-1}$, $E_0 = 5.53\pm^{0.44}_{0.38} \times 10^2$ GeV, $\Delta\gamma_1 = (-3.9\pm^{1.5}_{1.8}) \times 10^{-1}$, $E_1 = (9.8^{+3.2}_{-2.1}) \times 10^3$ GeV, and $s_1 \sim 90$. Though the hardening starts gradually around 550 GeV, the softening starts sharply around 10TeV. Therefore, the value of s_1 becomes high with a large uncertainty.

Figure 6 shows the energy dependence of the spectral index calculated within a sliding energy window. The spectral index is determined for each bin by a fit to the data including the neighboring $\pm$2 bins in the region below 20 TeV.
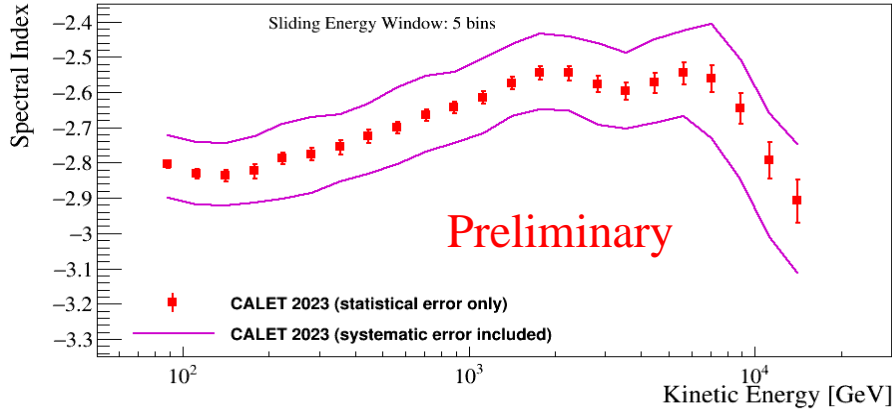

Figure 6*: Energy dependence of the spectral index calculated within a sliding energy window for CALET (red square). The spectral index is determined by fitting the data using 5 energy bins (the current bin $\pm$2 side bins within errors). The magenta lines show the uncertainty range including systematic errors.*

4. Discussion and summary

In the energy range from 50 GeV to 1 TeV, the CALET proton spectrum is consistent with AMS-02 and DAMPE. On the contrary, the spectrum from 1 TeV to 60 TeV is systematically lower than that of DAMPE by ~10%, though the difference is within the uncertainties. The spectral softening break energy observed with CALET ($9.8^{+3.2}_{-2.1}$ TeV) is consistent wihin the errors with that of DAMPE ($13.6^{+4.1}_{-4.8}$ TeV [5]). The observed spectral structure, hardening and softening, is a valuable input for modeling the mechanisms of cosmic-ray acceleration and propagation in the Galaxy.

We have successfully performed a precise measurement of the proton spectrum with CALET data taken from Oct. 2015 to Apr. 2023 with stable observations during more than seven years. We have observed a sharp spectral softening starting around 10 TeV. The spectral index changes from -2.6 to -2.9.

5. Acknowledgement

References

[1] O. Adriani *et al*. (CALET Collaboration), Phys. Rev. Lett. **122**, 181102 (2019).

[2] M. Aguilar *et al*. (AMS Collaboration), Phys. Rev. Lett. **114**, 171103 (2015).

[3] Y.S. Yoon *et al*. (CREAM-III Collaboration), Astrophys. J **839**, 5 (2017).

[4] O. Adriani *et al*. (CALET Collaboration), Phys. Rev. Lett. **129**, 101102 (2022).

[5] Q. An *et al*. (DAMPE Collaboration), Science Adv. **5**, eaax3793 (2019).

[6] Y. Asaoka *et al*. (CALET Collaboration), Astropart. Phys. **100**, 29 (2018)

[7] O. Adriani *et al*. (CALET Collaboration), Phys. Rev. Lett. **119**, 181101 (2017).

[8] O. Adriani *et al*. (CALET Collaboration), Phys. Rev. Lett. **120**, 261102 (2018).

[9] K. Kasahara, Proc. 24th Intl. Cosmic Ray Conf., Rome, Italy, ed. by N. Iucci and E. Lamanna (Intl. Union of Pure and Applied Phys. **1**, 399 (1995), http://adsabs.harvard.edu/full/1995ICRC....1..399K.

PoS(ICRC2023)092

Full Author List: CALET Collaboration

O.Adriani[1,2], Y. Akaike[3,4], K. Asano[5], Y. Asaoka[5], E. Berti[2,6], G. Bigongiari[7,8], W.R. Binns[9], M. Bongi[1,2], P. Brogi[7,8], A. Bruno[10], N. Cannady[11,12,13], G. Castellini[6], C. Checchia[7,8], M.L. Cherry[14], G. Collazuol[15,16], G.A. de Nolfo[10], K. Ebisawa[17], A.W. Ficklin[14], H. Fuke[17], S. Gonzi[1,2,6], T.G. Guzik[14], T. Hams[11], K. Hibino[18], M. Ichimura[19], K. Ioka[20], W. Ishizaki[5], M.H. Israel[9], K. Kasahara[21], J. Kataoka[22], R. Kataoka[23], Y. Katayose[24], C. Kato[25], N. Kawanaka[20], Y. Kawakubo[14], K. Kobayashi[3,4], K. Kohri[26], H.S. Krawczynski[9], J.F. Krizmanic[12], P. Maestro[7,8], P.S. Marrocchesi[7,8], A.M. Messineo[8,27], J.W. Mitchell[12], S. Miyake[28] A.A. Moiseev[29,12,13], M. Mori[30], N. Mori[2], H.M. Motz[18], K. Munakata[25], S. Nakahira[17], J. Nishimura[17], S. Okuno[18], J.F. Ormes[31], S. Ozawa[32], L. Pacini[2,6], P. Papini[2], B.F. Rauch[9], S.B. Ricciarini[2,6], K. Sakai[11,12,13], T. Sakamoto[33], M. Sasaki[29,12,13], Y. Shimizu[18], A. Shiomi[34], P. Spillantini[1], F. Stolzi[7,8], S. Sugita[33], A. Sulaj[7,8], M. Takita[5], T. Tamura[18], T. Terasawa[5], S. Torii[3], Y. Tsunesada[35,36], Y. Uchihori[37], E. Vannuccini[2], J.P. Wefel[14], K. Yamaoka[38], S. Yanagita[39], A. Yoshida[33], K. Yoshida[21], and W.V. Zober[9]

[1]Department of Physics, University of Florence, Via Sansone, 1 - 50019, Sesto Fiorentino, Italy, [2]INFN Sezione di Firenze, Via Sansone, 1 - 50019, Sesto Fiorentino, Italy, [3]Waseda Research Institute for Science and Engineering, Waseda University, 17 Kikuicho, Shinjuku, Tokyo 162-0044, Japan, [4]JEM Utilization Center, Human Spaceflight Technology Directorate, Japan Aerospace Exploration Agency, 2-1-1 Sengen, Tsukuba, Ibaraki 305-8505, Japan, [5]Institute for Cosmic Ray Research, The University of Tokyo, 5-1-5 Kashiwa-no-Ha, Kashiwa, Chiba 277-8582, Japan, [6]Institute of Applied Physics (IFAC), National Research Council (CNR), Via Madonna del Piano, 10, 50019, Sesto Fiorentino, Italy, [7]Department of Physical Sciences, Earth and Environment, University of Siena, via Roma 56, 53100 Siena, Italy, [8]INFN Sezione di Pisa, Polo Fibonacci, Largo B. Pontecorvo, 3 - 56127 Pisa, Italy, [9]Department of Physics and McDonnell Center for the Space Sciences, Washington University, One Brookings Drive, St. Louis, Missouri 63130-4899, USA, [10]Heliospheric Physics Laboratory, NASA/GSFC, Greenbelt, Maryland 20771, USA, [11]Center for Space Sciences and Technology, University of Maryland, Baltimore County, 1000 Hilltop Circle, Baltimore, Maryland 21250, USA, [12]Astroparticle Physics Laboratory, NASA/GSFC, Greenbelt, Maryland 20771, USA, [13]Center for Research and Exploration in Space Sciences and Technology, NASA/GSFC, Greenbelt, Maryland 20771, USA, [14]Department of Physics and Astronomy, Louisiana State University, 202 Nicholson Hall, Baton Rouge, Louisiana 70803, USA, [15]Department of Physics and Astronomy, University of Padova, Via Marzolo, 8, 35131 Padova, Italy, [16]INFN Sezione di Padova, Via Marzolo, 8, 35131 Padova, Italy, [17]Institute of Space and Astronautical Science, Japan Aerospace Exploration Agency, 3-1-1 Yoshinodai, Chuo, Sagamihara, Kanagawa 252-5210, Japan, [18]Kanagawa University, 3-27-1 Rokkakubashi, Kanagawa, Yokohama, Kanagawa 221-8686, Japan, [19]Faculty of Science and Technology, Graduate School of Science and Technology, Hirosaki University, 3, Bunkyo, Hirosaki, Aomori 036-8561, Japan, [20]Yukawa Institute for Theoretical Physics, Kyoto University, Kitashirakawa Oiwake-cho, Sakyo-ku, Kyoto, 606-8502, Japan, [21]Department of Electronic Information Systems, Shibaura Institute of Technology, 307 Fukasaku, Minuma, Saitama 337-8570, Japan, [22]School of Advanced Science and Engineering, Waseda University, 3-4-1 Okubo, Shinjuku, Tokyo 169-8555, Japan, [23]National Institute of Polar Research, 10-3, Midori-cho, Tachikawa, Tokyo 190-8518, Japan, [24]Faculty of Engineering, Division of Intelligent Systems Engineering, Yokohama National University, 79-5 Tokiwadai, Hodogaya, Yokohama 240-8501, Japan, [25]Faculty of Science, Shinshu University, 3-1-1 Asahi, Matsumoto, Nagano 390-8621, Japan, [26]Institute of Particle and Nuclear Studies, High Energy Accelerator Research Organization, 1-1 Oho, Tsukuba, Ibaraki, 305-0801, Japan, [27]University of Pisa, Polo Fibonacci, Largo B. Pontecorvo, 3 - 56127 Pisa, Italy, [28]Department of Electrical and Electronic Systems Engineering, National Institute of Technology (KOSEN), Ibaraki College, 866 Nakane, Hitachinaka, Ibaraki 312-8508, Japan, [29]Astroparticle Physics Laboratory, NASA/GSFC, Greenbelt, Maryland 20771, USA, [30]Department of Physical Sciences, College of Science and Engineering, Ritsumeikan University, Shiga 525-8577, Japan, [31]Department of Physics and Astronomy, University of Denver, Physics Building, Room 211, 2112 East Wesley Avenue, Denver, Colorado 80208-6900, USA, [32]Quantum ICT Advanced Development Center, National Institute of Information and Communications Technology, 4-2-1 Nukui-Kitamachi, Koganei, Tokyo 184-8795, Japan, [33]College of Science and Engineering, Department of Physics and Mathematics, Aoyama Gakuin University, 5-10-1 Fuchinobe, Chuo, Sagamihara, Kanagawa 252-5258, Japan, [34]College of Industrial Technology, Nihon University, 1-2-1 Izumi, Narashino, Chiba 275-8575, Japan, [35]Graduate School of Science, Osaka Metropolitan University, Sugimoto, Sumiyoshi, Osaka 558-8585, Japan, [36]Nambu Yoichiro Institute for Theoretical and Experimental Physics, Osaka Metropolitan University, Sugimoto, Sumiyoshi, Osaka 558-8585, Japan, [37]National Institutes for Quantum and Radiation Science and Technology, 4-9-1 Anagawa, Inage, Chiba 263-8555, Japan, [38]Nagoya University, Furo, Chikusa, Nagoya 464-8601, Japan, [39]College of Science, Ibaraki University, 2-1-1 Bunkyo, Mito, Ibaraki 310-8512, Japan